

Edge Weights and Network Properties in Multiple Sclerosis

Elizabeth Powell^{1,2}, Ferran Prados^{2,3}, Declan Chard^{2,4}, Ahmed Toosy², Jonathan D. Clayden⁵, and Claudia Gandini Wheeler-Kingshott^{2,6,7}

¹ Department of Medical Physics and Biomedical Engineering, University College London, UK

² Queen Square MS Centre, UCL Institute of Neurology, Faculty of Brain Sciences, University College London, UK

³ Centre for Medical Image Computing, Department of Medical Physics and Bioengineering, University College London, UK

⁴ National Institute for Health Research University College London Hospitals Biomedical Research Centre, UK

⁵ Developmental Imaging and Biophysics Section, Great Ormond Street Institute of Child Health, University College London, UK

⁶ Department of Brain and Behavioural Sciences, University of Pavia, Italy

⁷ Brain MRI 3T Center, IRCCS Mondino Foundation, Pavia, Italy

Abstract. Graph theory is able to provide quantitative parameters that describe structural and functional characteristics of human brain networks. Comparisons between subject populations have demonstrated topological disruptions in many neurological disorders; however interpreting network parameters and assessing the extent of the damage is challenging. The abstraction of brain connectivity to a set of nodes and edges in a graph is non-trivial, and factors from image acquisition, post-processing and network construction can all influence derived network parameters. We consider here the impact of edge weighting schemes in a comparative analysis of structural brain networks, using healthy control and relapsing-remitting multiple sclerosis subjects as test groups. We demonstrate that the choice of edge property can substantially affect inferences of network disruptions in disease, ranging from ‘primarily intact connectivity’ to ‘complete disruption’. Although study design should predominantly dictate the choice of edge weight, it is important to consider how study outcomes may be affected.

Keywords: graph theory · network · edge weight · graph property · connectivity · permutation · multiple sclerosis.

1 Introduction

The brain is a complex network of grey matter nuclei densely interconnected by axon bundles. Communication between these cortical regions is the foundation of brain function, and damage to the connecting axon bundles is thought to cause a range of neurological disorders [1, 2]; techniques for estimating axonal damage

and characterising grey matter interactions could therefore offer considerable opportunities in advancing our understanding of brain structure and function in neurological diseases.

The application of graph theory to this network representation of the human brain is a valid step towards mapping connectivity: cortical regions and their pairwise interactions can be considered as nodes (vertices) and edges, with edge weights describing some structural or functional property of the connection between regions. Graph theoretic analysis has consistently demonstrated non-random features in human brain graphs, including small-world organisation and modularity [3, 4], as well as network disruptions in a variety of neurological disorders [5, 6]. Moreover, it is possible to characterise aspects of network topology at different levels, for example at both local (nodal) and global (whole network) levels.

The technique is not without its challenges, though. The choice of vertices and edges inherently dictates the derived network properties, even to the extent that parcellation strategy [7] and tractography algorithm [8] have a demonstrable effect. Naturally, edge weights also influence derived network measures [9].

Appropriate edge weighting strategies are widely discussed [10, 11]. For the structural connectome - defined as spatially distinct cortical regions connected by axon bundles reconstructed using diffusion tensor imaging (DTI) - typical edge weights include the number of streamlines (NSL) connecting pairwise regions, the mean fractional anisotropy (FA) of the tract, and binary values. All are valid weighting schemes: the NSL and FA offer some suggestion of connection ‘integrity’ or ‘efficiency’, while binary graphs provide analytic simplicity.

Network parameters are known to vary as a result of the chosen weighting scheme [12]; however the extent to which this variability may affect a comparative analysis of networks between groups is not obvious.

The purpose of this study was to evaluate the impact of the edge weighting scheme on intergroup network differences in order to generalise results and highlight possible confounding factors. We perform an analysis of global and local network properties using healthy control (HC) and relapsing-remitting multiple sclerosis (RRMS) subject groups as test sets, and implement a robust permutation-based approach for statistical hypothesis testing that is novel in this context.

2 Methods

2.1 Participants

Twenty seven healthy controls (HC) (16 female; mean age 37 ± 12 years) and 33 RRMS patients (24 female; mean age 40 ± 10 years; median EDSS score 2.0) were recruited; written consent was obtained for all subjects. No significant age or gender differences were observed between groups ($p = 0.27$ and $p = 0.28$ respectively).

2.2 MRI Acquisition and Pre-Processing

Images were acquired using a 3T MRI system (Philips Healthcare, Best, Netherlands) with a 32-channel head coil. Diffusion-weighted image (DWI) volumes were acquired with diffusion weighting along 61 directions and $b = 1200 \text{ s/mm}^2$, plus 7 volumes with $b = 0 \text{ s/mm}^2$, with resolution $2 \times 2 \times 2 \text{ mm}^3$, TR = 24000 s and TE = 68 s. A 3D T₁-weighted fast field echo with resolution $1 \times 1 \times 1 \text{ mm}^3$, TR = 6.9 s, TE = 3.1 s and inversion time TI = 824 s was also acquired on each participant.

All DWI were corrected for eddy current [13], motion and susceptibility distortions [14] in native space. The T₁-weighted images were registered [14] to the corrected DWI and parcellated [15] into structurally-defined sub-regions.

Estimates of fibre orientation were obtained from a fit of the ball-and-sticks model to the DWI [16]; a maximum of 3 fibres were modelled per voxel. Probabilistic tractography [17] was performed using 1000 streamline seeds in each white matter voxel. The DTI-derived average FA for each reconstructed tract was also calculated [17].

2.3 Network Reconstruction

Network vertices were defined as the 98 cortical regions identified by the anatomical parcellation. For brevity, each vertex was assigned a number from 1-98 such that the set of vertices was given by $V = \{v_1, v_2, \dots, v_n\}$, with $n = 98$. Correspondences with anatomical regions are given in Table 1.

Association matrices were generated [17] for each subject and masked to remove any edges absent in more than N subjects, where $N = \max(N_{\text{HC}}, N_{\text{RRMS}}) + 2$ and $N_{\text{HC}}, N_{\text{RRMS}}$ denote HC and RRMS group sizes respectively. Masking in this way ensured that any given edge was present in at least two subjects within a group and aided the statistical analysis. All vertices remained connected for all subjects.

Edges were weighted using four different metrics commonly reported: the NSL, the NSL corrected for tract length (NSL_{cor}), the mean tract FA, and a simple binary weight. The correction for tract length was implemented as the product of the NSL connecting two regions and the average length of those streamlines. An example of each association matrix generated for a single subject is provided in Fig. 1.

2.4 Statistical Analysis

Global and local network properties were calculated [17] for each subject and edge weighting scheme. The global metrics evaluated were efficiency, mean shortest path and modularity; the local properties were efficiency, clustering coefficient, node strength and betweenness centrality.

Significant differences in global network properties between HC and RRMS groups were identified using a t-test ($p < 0.05$).

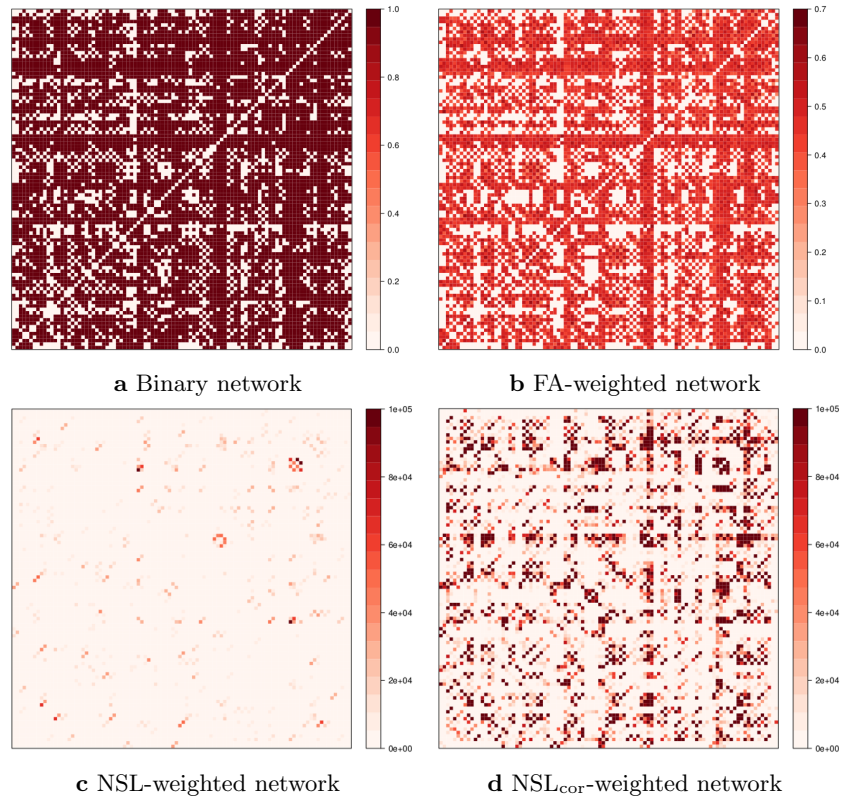


Fig. 1 Example network types generated for a single subject. **a** Binary network, **b** Network weighted using average tract FA, **c** Network weighted using the NSL, **d** Network weighted using the NSL corrected for tract length

Table 1 Correspondences between anatomical regions and vertex number

Right	Left	Anatomical region	49	50	
			51	52	middle temporal gyrus
1	2	anterior cingulate gyrus	53	54	occipital pole
3	4	anterior insula	55	56	occipital fusiform gyrus
5	6	anterior orbitofrontal cortex	57	58	pars opercularis
7	8	angular gyrus	59	60	pars orbitalis
9	10	calcarine cortex	61	62	posterior cingulate gyrus
11	12	central operculum	63	64	precuneus
13	14	cuneus	65	66	parahippocampal gyrus
15	16	entorhinal cortex	67	68	posterior insula
17	18	frontal operculum	69	70	parietal operculum
19	20	frontal pole	71	72	postcentral gyrus
21	22	fusiform gyrus	73	74	posterior orbitofrontal cortex
23	24	gyrus rectus	75	76	planum polare
25	26	inferior occipital gyrus	77	78	precentral gyrus
27	28	inferior temporal gyrus	79	80	planum temporale
29	30	lingual gyrus	81	82	subcallosal area
31	32	lateral orbitofrontal cortex	83	84	superior frontal gyrus
33	34	middle cingulate gyrus	85	86	supplementary motor cortex
35	36	medial frontal cortex	87	88	supramarginal gyrus
37	38	middle frontal gyrus	89	90	superior occipital gyrus
39	40	middle occipital gyrus	91	92	superior parietal lobule
41	42	medial orbitofrontal gyrus	93	94	superior temporal gyrus
43	44	medial postcentral gyrus	95	96	temporal pole
45	46	medial precentral gyrus	97	98	pars triangularis
47	48	medial superior frontal gyrus			transverse temporal gyrus

Significant intergroup differences in local network properties were determined using a permutation-based approach. This strategy enabled the null distribution of p values to be empirically derived whilst taking multiple comparisons into consideration, from which a corrected p value could be estimated. Separate null distributions of p values were generated for each network type and property.

At each permutation, then, group labels were randomly reallocated to create new ‘HC’ and ‘RRMS’ groups; original group sizes were preserved in each of the 1000 samples generated. At each node the mean local network properties were compared between sample groups using a t-test. The minimum p value obtained across all node comparisons at each permutation was added to the null distribution for a given weighting scheme and network property; the procedure was then that of a step-down ‘minimum p ’ approach [18]. The family-wise Type I error rate was subsequently controlled for in the strong sense.

Table 2 Global network differences between HC and RRMS subject groups

Edge weight	Global efficiency	Mean shortest path	Modularity
FA	HC > MS, $p < 0.001$	HC < MS, $p = 0.002$	-
NSL _{cor}	HC > MS, $p < 0.001$	HC < MS, $p = 0.008$	-
NSL	HC > MS, $p = 0.022$	HC < MS, $p = 0.017$	-
Binary	-	-	HC > MS, $p = 0.047$

3 Results

3.1 Intergroup Differences in Global Network Properties

Global efficiency was significantly lower ($p < 0.05$) in RRMS patients relative to HC subjects in networks weighted using FA, NSL_{cor} and NSL edge properties; the mean shortest path was correspondingly greater ($p < 0.05$) in the RRMS population across the same networks. Binary networks exhibited no intergroup differences in global efficiency and mean shortest path; however modularity was significantly greater in the HC group ($p < 0.05$).

These results are consistent with published findings [19, 20]. Of note here is that inferences of intergroup differences in global network properties were unaffected by the choice of edge property for weighted networks, but were substantially different between weighted and binary networks.

3.2 Intergroup Differences in Local Network Properties

Local Efficiency. Lower nodal efficiencies were observed in the RRMS cohort across all weighted networks, which is consistent with published reports [19]; no alterations were detected in binary networks (Fig. 2a). However, the set of vertices with different efficiency properties between groups was highly inconsistent across the weighted network types. FA-weighted networks exhibited the greatest intergroup differences, with lower efficiency in 97 out of 98 nodes in the RRMS cohort ($p < 0.05$, corrected). In NSL_{cor}-weighted networks only 78 nodes demonstrated alterations between groups ($p < 0.05$, corrected), while in NSL-weighted networks the proportion was lower still at just 12 nodes ($p < 0.05$, corrected).

The variation in findings between the NSL_{cor}- and NSL-weighted networks was particularly striking. It is possible here that additional uncertainties in NSL-weighted networks, resulting from inherent biases in probabilistic tractography towards tract length [21], could be driving the discrepancies.

Clustering Coefficient. Lower clustering coefficients were observed in the RRMS group in all weighted networks (Fig. 2b), in line with previous studies [19]. The extent of the alterations was again highly variable between the weighted network types: substantially more intergroup differences were identified in FA-weighted networks (54 out of 98 nodes; $p < 0.05$, corrected) than in NSL_{cor}- and NSL-weighted networks (5 and 4 nodes respectively; $p < 0.05$, corrected). No differences were observed in binary networks.

Nodal Strength. Lower nodal strengths were found in the RRMS group in FA-weighted, NSL_{cor} -weighted and binary networks (Fig. 2c), consistent with published findings [19]. The proportion of nodes exhibiting different strength properties between the HC and RRMS groups once more varied across the network types, with 14 out of 98 nodes ($p < 0.05$, corrected) identified in FA-weighted networks, 4 nodes ($p < 0.05$, corrected) in NSL_{cor} -weighted networks and 1 node ($p < 0.05$, corrected) in binary networks. No intergroup differences were observed in NSL-weighted networks.

Betweenness Centrality. Minimal intergroup differences were observed in betweenness centrality: only 2 nodes in FA-weighted networks displayed significantly greater ($p < 0.05$, corrected) betweenness centrality in the RRMS group (Fig. 2d). No other networks indicated any differences.

4 Discussion

We have explicitly demonstrated the impact of the edge weighting scheme on a comparative analysis of network properties using HC subjects and RRMS patients with very mild disease severity as example data sets. While graph theoretic analyses performed over different network types will be naturally incongruent to a degree, the disparities presented here are striking. Given any one of the network types in isolation, as is common in connectivity studies, the assessment of damage to the structural connectome of these RRMS patients would be substantially different, with potential conclusions ranging from ‘intact connectivity’ to ‘complete disruption despite the mild disability’.

In FA-weighted networks, for example, reductions were observed in the local efficiency of almost every node and in the clustering coefficient of more than half the nodes. Further, regions of the default mode network (DMN) - which is important for high level function and prone to impairment in MS [22] - such as the precuneus and posterior cingulate gyrus displayed significantly reduced nodal strength. From these findings it may be inferred that the networks of these RRMS patients were substantially damaged despite the relatively mild disability levels (the median EDSS was just 2.0, indicating no major motor, visual, sensory or cognitive disabilities), and that the graph properties were in fact sensitive to subtle MS pathology.

In NSL_{cor} -weighted networks, on the other hand, the clustering coefficient, node strength and betweenness centrality were unaffected in the majority of nodes, and core DMN nodes in particular showed no changes; only local efficiency appeared to indicate any alterations. It may be concluded here, then, that networks in this RRMS cohort were only moderately disrupted, and potentially reflected their relative lack of clinical disability.

Evidently, interpretations of network analyses must be made with caution: graph theoretic metrics may be sensitive to subtle alterations between groups but they lack biological specificity. Factors known to systematically bias estimates of structural connectivity range from head motion [23] and low signal-to-noise ratio

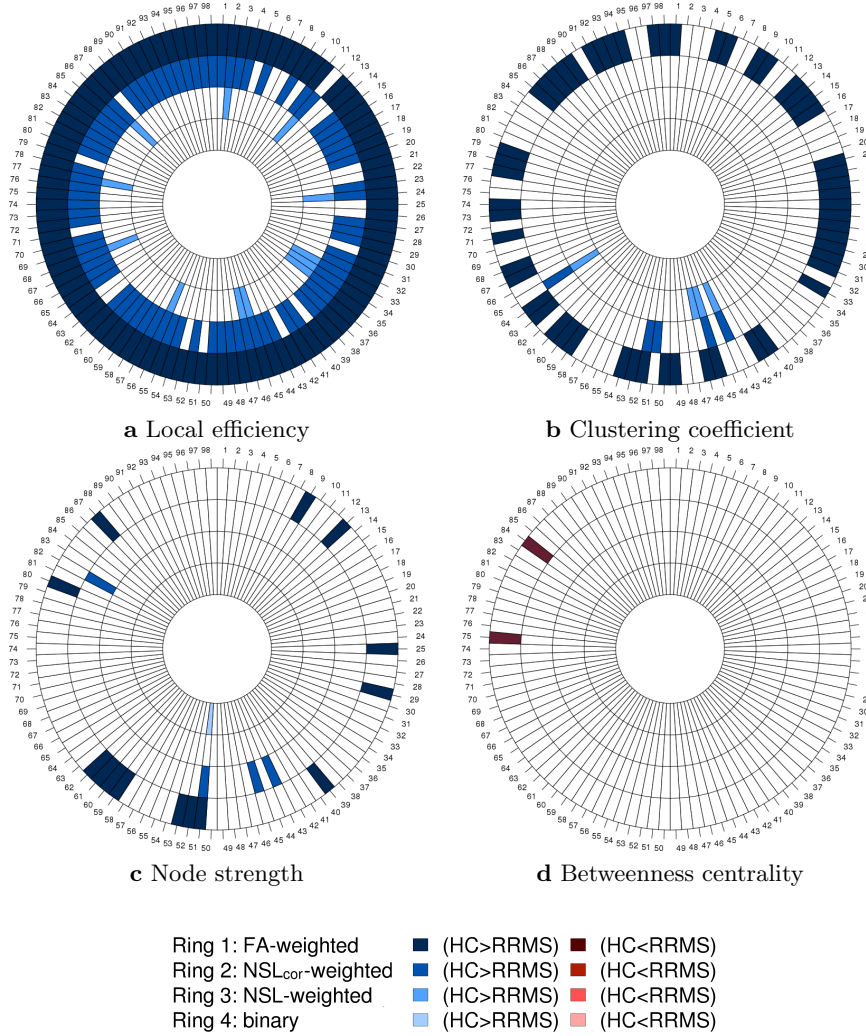


Fig. 2 Significant intergroup differences ($p < 0.05$, corrected) in local network properties. **a** Local efficiency, **b** Clustering coefficient, **c** Node strength, **d** Betweenness centrality. Each numbered segment corresponds to a node, as specified in Table 1. In each sub-figure the concentric rings correspond to specific network types: the outermost ring (ring 1) corresponds FA-weighted graphs; ring 2 to NSL_{cor}-weighted networks; ring 3 to NSL-weighted networks; ring 4 (innermost ring) to binary networks. The colour indicates whether the network property is significantly greater in HC subjects (blue) or RRMS patients (red)

[24] during acquisition to the parcellation strategy and tractography algorithm adopted during image processing. This study highlights for the first time how outcomes in intergroup comparative studies across different network types may be affected by the combined influence of biological alterations and factors unrelated to inter-regional connectivity. Specifically, comparisons of local network properties between groups may be particularly prone to variations across network types. The global metrics evaluated here were comparatively less sensitive to weighting scheme; however the utility of global properties is limited by a lack of specificity to potentially more meaningful local alterations.

The relative absence of intergroup differences both locally and globally in binary networks is likely to reflect the similarity in edge set between groups, and the applied edge threshold is likely to be influential here. A complete analysis of individual edges was beyond the scope of this work, but could be considered in future studies.

The specificity of local network properties to biological alterations may be improved to a degree by including appropriate confounding variables, such as estimates of head motion, as covariates in the statistical analysis [23]. This study was designed to reflect conventional connectivity papers and so did not incorporate such covariates in the analysis; however the permutation testing implemented here can be easily extended to include covariates. Moreover, it is a powerful and robust approach for controlling multiple correlated comparisons that is novel in this context, and would be beneficial in comparative studies of the same nature. In particular, it could be interesting to compare local network properties in alternative subject populations, such as those with more severe pathology: substantial microstructural changes may then outweigh confounding factors and result in more consistent outcomes.

Ultimately, the choice of edge weight is largely dependent on the study design in question. It is important to consider, though, that the nuances of each weighting scheme influence derived network parameters, which may in turn substantially impact outcomes in intergroup comparative studies.

5 Conclusions

Network-based approaches offer important contributions towards analysing the connections that form the basis of brain structure and function; however the interpretation of graph theoretic properties remains challenging. We demonstrate, using HC and RRMS subjects as test populations, that the choice of edge weight in intergroup comparisons is non-trivial and can substantially affect inferences of network disruptions in disease. Study design should primarily drive the choice of weighting scheme, but potential confounding factors and interpretation pitfalls must be considered.

Acknowledgements

The NMR unit where this work was performed is supported by grants from the Multiple Sclerosis Society of Great Britain and Northern Ireland, Philips Healthcare, and supported by the UCL/UCLH NIHR (National Institute for Health Research) BRC (Biomedical Research Centre).

Bibliography

- [1] Geschwind, N.: Disconnexion syndromes in animal and man: Part I. *Brain*. **88** (1965) 237–294
- [2] Geschwind, N.: Disconnexion syndromes in animal and man: Part II. *Brain*. **88** (1965) 237–294
- [3] Bassett, D.S., Bullmore, E.: Small-world brain networks. *Neuroscientist*. **12**(6) (2006) 512–523
- [4] van den Heuvel, M.P., Sporns, O.: Rich-club organization of the human connectome. *J. Neurosci.* **31**(44) (2011) 15775–15786
- [5] Bassett, D.S., Bullmore, E., Verchinski, B.A., Mattay, V.S., Weinberger, D.R., Meyer-Lindenberg, A.: Hierarchical organization of human cortical networks in health and schizophrenia. *J. Neurosci.* **28**(37) (2008) 9239–9248
- [6] He, Y., Dagher, A., Chen, Z., Charil, A., Zijdenbos, A., Worsley, K., Evans, A.: Impaired small-world efficiency in structural cortical networks in multiple sclerosis associated with white matter lesion load. *Brain*. **132**(12) (2009) 3366–3379
- [7] Zalesky, A., Fornito, A., Harding, I.H., Cocchi, L., Yücel, M., Pantelis, C., Bullmore, E.T.: Whole-brain anatomical networks: does the choice of nodes matter? *Neuroimage*. **50**(3) (2010) 970–983
- [8] Bastiani, M., Shah, N., Goebel, R., Roebroeck, A.: Human cortical connectome reconstruction from diffusion weighted MRI: the effect of tractography algorithm. *Neuroimage*. **62**(3) (2012) 1732–1749
- [9] Rubinov, M., Sporns, O.: Complex network measures of brain connectivity: uses and interpretations. *Neuroimage*. **52** (2010) 1059–1069
- [10] Fornito, A., Zalesky, A., Breakspear, M.: Graph analysis of the human connectome: promise, progress, and pitfalls. *Neuroimage*. **80** (2013) 426–444
- [11] Bullmore, E.T., Sporns, O.: Complex brain networks: graph theoretical analysis of structural and functional systems. *Nature Rev. Neurosci.* **10** (2009) 186–98
- [12] Cheng, H., Wang, Y., Sheng, J., Kronenberger, W.G., Mathews, V.P., Hummer, T.A., Saykin, A.J.: Characteristics and variability of structural networks derived from diffusion tensor imaging. *Neuroimage*. **61**(4) (2012) 1153–1164
- [13] Andersson, J., Sotiropoulos, S.N.: An integrated approach to correction for off-resonance effects and subject movement in diffusion MR imaging. *Neuroimage*. **125** (2015) 1063–1078
- [14] Bhushan, C., Haldar, J.P., Joshi, A.A., Leahy, R.M.: Correcting susceptibility-induced distortion in diffusion-weighted MRI using constrained nonrigid registration. In: *APSIPA ASC*. (2012) 1–9
- [15] Cardoso, M., Modat, M., Wolz, R., Melbourne, A., Cash, D., Rueckert, D., Ourselin, S.: Geodesic information flows: spatially-variant graphs and their

- application to segmentation and fusion. *IEEE Trans. Med. Imaging.* **34**(9) (2015) 1976–1988
- [16] Behrens, T., Berg, H., Jbabdi, S., Rushworth, M.F., Woolrich, M.: Probabilistic diffusion tractography with multiple fibre orientations: what can we gain? *Neuroimage.* **34**(1) (2007) 144–155
- [17] Clayden, J., Mu, S., Storkey, A., King, M., Bastin, M., Clark, C.: TractoR: magnetic resonance imaging and tractography with R. *J. Stat. Softw.* **44**(8) (2011) 1–18
- [18] Westfall, P., Young, S.: Resampling-based multiple testing: examples and methods for p-value adjustment. Wiley. (2003)
- [19] Shu, N., Duan, Y., Xia, M., Schoonheim, M.M., Huang, J., Ren, Z., Sun, Z., Ye, J., Dong, H., Shi, F.D., Barkhof, F., Li, K., Liu, Y.: Disrupted topological organization of structural and functional brain connectomes in clinically isolated syndrome and multiple sclerosis. *Sci. Rep.* **6** (2016)
- [20] Llufriu, S., Martinez-Heras, E., Solana, E., Sola-Valls, N., Sepulveda, M., Blanco, Y., Martinez-Lapiscina, E.H., Andorra, M., Villoslada, P., Prats-Galino, A., Saiz, A.: Structural networks involved in attentional function in multiple sclerosis. *Neuroimage. Clin.* **13** (2017) 288–296
- [21] Zalesky, A., Fornito, A.: A DTI-derived measure of cortico-cortical connectivity. *IEEE Trans Med. Imaging.* **28**(7) (2009) 1023–1036
- [22] Gamboa, O.L., Tagliazucchi, E., Von Wegner, F., Jurcoane, A., Wahl, M., Laufs, H., Ziemann, U.: Working memory performance of early MS patients correlates inversely with modularity increases in resting state functional connectivity networks. *Neuroimage.* **94** (2014) 385–395
- [23] Baum, G.L., Roalf, D.R., Cook, P.A., Ciric, R., Rosen, A.F.G., Xia, C., Elliott, M.A., Ruparel, K., Verma, R., Tunç, B., Gur, R.C., Gur, R.E., Bassett, D.S., Satterthwaite, T.D.: The impact of in-scanner head motion on structural connectivity derived from diffusion MRI. *Neuroimage.* **173** (2018) 275–286
- [24] Jones, D.K., Knösche, T.R., Turner, R.: White matter integrity, fiber count, and other fallacies: the do’s and don’ts of diffusion MRI. *Neuroimage.* **73** (2013) 239–254